Calculation and Evaluation of Proton-Induced Reactions on N, O, Zn, and Cd up to 50 MeV

Doohwan Kim[1], Yong-Deok Lee, Young-Ouk Lee and Jonghwa Chang
Korea Atomic Energy Research Institute

ABSTRACT

We have evaluated the proton-induced nuclear data of N, O, Zn and Cd for energies between 0.5 and 50 MeV. The purpose of this work is to examine the applicability of the optical potential parameters in RIPL(Reference Input Parameter Library for theoretical calculations of nuclear reactions) of IAEA. We apply the ECIS96-GNASH nuclear model code, which includes Hauser-Feshbach, preequilibrium and direct reaction mechanisms. The evaluated reaction cross sections are compared with the experimental data obtained from EXFOR at the NEA Data Bank, and stored in MF3 and MF6 of the ENDF-6 format.

I.   Introduction

Medical radioisotopes are used for diagnostic and therapeutic purposes, as well as for metabolism and physiological function research in modern medicine. If a short-lived radioisotope emits a predominant or single gamma-ray of 60-300 keV, it is of great advantage, since single proton emission computer tomograph (SPECT) can be performed; similarly, positron emitters are also of great significance since three dimensional high resolution scans can be obtained via positron emission tomography (PET). Some of the radioisotopes find therapeutic applications, especially if they emit alpha or high energy electrons, or Auger electrons. Nuclear data relevant to medically important radioisotopes can be divided into two major categories: the decay data and nuclear reaction cross sections. The former is of prime importance in deciding upon the suitability of a radioisotope for medical application, and the latter is of great significance regarding the production and radionuclidic quality control of the desired radioisotope. In general, the decay data are known with sufficient accuracy, but the reaction cross sections need more attention, especially charged particle nuclear data (CPND), because they are scarce and scattered [1].

In the nuclear reaction for medical radioisotope production, the unwanted isotopes are parasitically produced by minor reaction channels. The purpose of this work is to evaluate these unwanted isotope cross sections. In the previous work, we evaluated and fitted many charged particle induced reactions, such as ^{14}N(p,α)^{11}C, ^{14}N(d,n)^{15}O, ^{16}O(p,α)^{13}N, ^{18}O(p,n)^{18}F, ^{68}Zn(p,2n)^{67}Ga, ^{68}Zn(p,3n)^{66}Ga, ^{67}Zn(p,n)^{67}Ga, ^{67}Zn (p,2n) ^{66}Ga, ^{66}Zn(p,n)^{66}Ga, ^{66}Zn(p,X) ^{65}Zn, ^{nat}Zn(p,X)^{66}Ga, ^{nat}Zn(p,X)^{67}Ga and ^{112}Cd (p,2n) ^{111}In reactions, with the experimental data [1]. In this work, we have evaluated the proton-induced nuclear data of ^{14}N, ^{16}O, ^{18}O, ^{nat,64,66,67,68}Zn and ^{112}Cd for energies between 0.5 and 50 MeV by the ECIS96-GNASH code system [2]. The evaluated reaction cross sections are compared with the experimental data obtained from EXFOR at the NEA Data Bank, and stored in MF3 and MF6 of the ENDF-6 format.

---

[1]E-mail:dookim@lui.kaeri.re.kr

Section 2 explains the ECIS-GNASH code system and the role of each code. Section 3 describes the optical potential parameters and the input data-files for the ECIS96-GNASH calculation. In section 4, finally, we show our evaluated results and summarize conclusions.

II.   ECIS-GNASH Code System

ECIS-GNASH code system enables us to fulfill the nuclear model calculations automatically, and to preserve the evaluated results in the ENDF6-datafile by "gnscript". We need the mass table and the level scheme table to perform this code system. ECIS96-GNASH consists of ECIS96 and GNASH code as well as several auxiliary codes, such as PREGNASH, POSTECIS, POST-GNASH and MINGUS3[3]. The present configuration of the code permits the following incident particle types, such as neutron, proton, deteron, triton, ^{3}He and ^{4}He, in energies up to 50 MeV. As incident particle and target nuclei are given in PREGNASH.INP, the emitting particles are determined and then five particle types are chosen: neutron, proton, deuteron, triton and ^{4}He. In PREGNASH.INP, nkim,pkim,dkim,tkim and akim are the subroutines to include the optical potential parameters of neutron, proton, deuteron, triteron and alpha-particle, respectively. The "gnscript" is the modular file that describes the process carried out automatically. PREGNASH generates input files for ECIS96 and GNASH.

ECIS ("*Equations Couplees en Iterations Sequentielles*") was introduced to solve coupled channel problems in the optical potential model calculations and the direct reaction obtained from the continuous states in the intermediate energy region with the Dirac as well as the Schrödinger equation [4, 5]. We used the relativistic quantum mechanical dynamics for running ECIS96 code. There are three input-files for ECIS96 : ecincid.inp, ectrans.inp and ecdisc.inp. The input file "ecincid.inp" is for calculating the total, elastic and reaction cross sections and the differential cross section with respect to elastic angle distributions. The "ectrans.inp" is for calculating the transmission coefficients which are necessary for GNASH run. The "ecdisc.inp" enables ECIS96 to calculate the inelastic cross section by using DWBA theory. All calculated results become the input of GNASH and are stored in tape10 and tape33 . POSTECIS transforms the ECIS96 results into GNASH input format.

GNASH code uses not only the quantum mechanical statistical model, the Hauser-Feshbach model, in order to take into account the chain reaction effect in the compound nucleus, but also the semi-classical exciton model to determine the pre-equilibrium spectra of the emitting particles. The code has been used for calculations at energies as low as 0.1 keV and as high as 100 MeV. The models utilized are expected to be most applicable for the energy range 1 keV to 50 MeV. In order to take into account the transmission and the effect for the direct reaction, GNASH needs auxiliary codes, such as SCAT, DWUCK and ECIS, and we choose ECIS.

The γ-ray transmission coefficients were obtained by the Kopecky-Uhl model [6]. In Table 1, EG1 and GG1 are the position and width of the first peak, which is the giant dipole resonance (GDR), and EG2 and GG2 represent the position and width of the second peak [7]. POSTGNASH transforms the GNASH output into data for MINGUS3.

MINGUS3 generates the ENDF6-format file from the ECIS and GNASH results. The original code was modified to handle the individual reaction cross sections in MF=3 as well as the residual reaction cross sections in MF=6. The endf6.inp is the input file of MINGUS3.

III.   Model Calculations

1.   General

The nucleon-nucleus optical model provides the foundation of theoretical analyses and evaluations of nuclear cross sections that are used in making nuclear data for applications. In addition to offering a convenient means for the calculation of reaction, shape elastic and total cross sections, optical model potentials are widely used in quantum mechanical pre-equilibrium and direct-reaction theory calculations and, most importantly, in supplying particle transmission coefficients for Hauser-Feshbach statistical-theory analyses used in nuclear data evaluations. The importance of optical model parameterizations is made even more apparent by the worldwide diminution of experimental facilities for low-energy nuclear physics measurements and the consequent increased reliance on theoretical methods for providing nuclear data for applications. Therefore, the preservation of past work aimed at describing experimental results with optical model potentials is vital for the future development of nuclear data bases [8].

Actually, it is impossible to solve the complicated many-body problem of the scattering of a nucleon from a nucleus, because it is difficult to know the interaction between an incident nucleon and a nucleon in the target and the medium effect occurring due to some collisions. One approach to resolve the scattering problems is to introduce a complex one-body potential, called optical potential, and to make the nucleon-nucleus optical model that is regarded as the scattering of single particle from a complex one whose shape is determined by the optical potential parameters[9]. A global nucleon-nucleus optical model potential has parameters that are the smooth function of target A and Z, projectile type (proton and neutron), and laboratory bombarding energy (E) and it describes data over a wide range of these variables. Therefore, the determination of these parameters is based on the global experimental results and theoretical ones[10].

The evaluations are based mainly on model calculations using the ECIS96-GNASH code system. Optical model calculations were performed with ECIS96 and when evaluating pre-equilibrium cross sections, we also considered exciton model results from the GNASH code [11], and continuum level densities proposed by Ignatyuk [12]. The calculations provide a useful way to interpolate and extrapolate to other energies. Model calculations enable evaluated libraries to be generated for all reaction products in a fully consistent way.

A typical representation of the optical model potential is the following:

$$
\begin{aligned}
V(r) = \quad & - \quad V_V f_R(r) - iW_V f_V(r) + 4ia_D W_D \frac{df_D(r)}{dr} \\
& + \quad \frac{\lambda^2}{r}[V_{SO}\frac{df_{VSO}(r)}{dr} + iW_{SO}\frac{(df_{WSO}(r))}{dr}]\sigma \cdot l
\end{aligned}
$$

where λ^2 is the pion Compton wavelength squared (≈ 2) and the form factors are of the standard Woods-Saxon form: $f_i(r) = \frac{1}{1+exp[(r-R_i)/a_i]}$. These parameters are obtained from RIPL[8], and the kind of optical potentials used in this work are listed in Table 2. The values in Table 2 indicate the index of RIPL for the optical parameters. Figures 2-4 show the resulting potential depths of the real and imaginary volumes and the imaginary surface as a function of both neutron and proton energies. The potential depths for protons are shown to be higher than that of neutrons. The discontinuities appear in the potential depths for ^{14}N, because there are several kind of optical potentials for several incident energy ranges.

2. Proton induced reaction on ^{14}N and ^{16}O

Zhuang fitted and evaluated the reaction data on ^{14}N(p,α)^{11}C, ^{14}N(d,n)^{15}O and ^{16}O(p,α)^{13}N [1]. Several experimental data are introduced from EXFOR at the NEA Data Bank to verify the appropriateness of the optical potential parameters obtained from RIPL without any modification of them. Optical potentials for protons and neutrons were taken from Chadwick *et*

al.[13, 14] in Table 3. Potentials for the other ejectiles are also needed for calculating transmission coefficients for their decay. Potentials for α-particles, deuterons and ^{3}He were referenced to Avrigeanu *et al.*[15], Bojowald *et al.*[16] and Becchetti *et al.*[17], respectively. The same α-particle and deuteron optical parameters are applied to ^{14}N, ^{16}O, ^{18}O, ^{nat,64,66,67,68}Zn and ^{112}Cd, since they can be used in wide mass and energy regions which we have evaluated. According to Table 2, the potential for emitting ^{3}He is used here instead of the one for emitting tritons, since the production cross sections including ^{3}He are larger than those including triton, and there exist few experimental data for ^{3}He. The production cross sections below 0.1mb were neglected.

3. Proton induced reaction on ^{18}O

Zhuang fitted and evaluated the reaction data on ^{18}O(p,n)^{18}F [1]. Potentials for protons and neutrons were referenced to Menet *et al.*[18] and Igarasi [19], respectively, as listed in Table 4.

4. Proton induced reaction on ^{nat,64,66,67,68}Zn and ^{112}Cd

Zhuang fitted and evaluated the reaction data on ^{nat}Zn(p,X)^{66}Ga, ^{nat}Zn(p,X)^{67}Ga, ^{66}Zn(p,n) ^{66}Ga, ^{66}Zn(p,X)^{65}Zn, ^{67}Zn(p,n)^{67}Ga, ^{67}Zn(p,2n)^{66}Ga, ^{68}Zn(p,2n)^{67}Ga, ^{68}Zn(p,3n)^{66}Ga and ^{112}Cd (p,2n) ^{111}In [1]. Potentials for protons and neutrons were referenced to Varner *et al.*[10], whose optical potential forms are given as following :
Real central potential:

$$
\begin{aligned}
V_r &= V_0 \pm V_t \frac{N-Z}{A} + (E - E_c)V_e \Longrightarrow + : \text{protons}, - : \text{neutrons}, \\
R_0 &= r_0 A^{\frac{1}{3}} + r_0^{(0)}, \\
E_c &= \frac{6Ze^2}{5R_c} = \frac{1.73Z}{R_c} MeV, for(p,p),
\end{aligned}
$$

Coulomb potential radius:

$$
R_c = r_c A^{\frac{1}{3}} + r_c^{(0)} = 1.238 A^{\frac{1}{3}} + 0.116 fm.
$$

Spin-orbit potential:

$$
R_{so} = r_{so} A^{\frac{1}{3}} + r_{so}^{(0)}.
$$

Imaginary central potential:

$$
\begin{aligned}
W_v &= W_{v0}[1 + exp(\frac{W_{ve0} - (E - E_c)}{W_{vew}})]^{-1}, \\
W_s &= (W_{s0} \pm W_{st} \frac{N_Z}{A})[1 + exp(\frac{(E - E_c) - W_{se0}}{W_{sew}}]^{-1}, \\
R_w &= r_w A^{\frac{1}{3}} + r_w^{(0)}
\end{aligned}
$$

The parameter values with uncertainties are given in Table 5. Natural Zn consists of five isotopes, i.e. ^{64}Zn in 48.6 %, ^{66}Zn in 27.9%, ^{67}Zn in 4.1%, ^{68}Zn in 18.8% and ^{70}Zn in 0.6% [20]. The production cross sections for ^{70}Zn are ignored, since the one for ^{70}Zn is negligible. We chose the same optical potential for all Zn-isotopes.

IV. Results and Conclusion

Figures 1-8 summarize our evaluation results of ^{14}N, ^{16}O, ^{18}O, ^{nat,64,66,67,68}Zn and ^{112}Cd isotopes. In Fig. 1-2, the calculated results for ^{14}N (p,α) ^{11}C and ^{16}O (p,α) ^{13}N reaction cross sections are compared with the experimental data taken from the calculation notes of Zhuang [1]. The calculated results show that the overall shape and magnitude of (p,α) reaction cross sections are in agreement with the experimental data and around 7MeV there exist the peak shapes of the experimental data which can hardly be explained in our work. Our evaluations with different sets of optical potential parameters for several energy regions from RIPL also give discontinuities of transmission coefficients and cross sections at boundary energies. The comparison of calculated results with the experimental data for the ^{18}O (p,n) ^{18}F reaction cross section are given in Fig 3. This discrepancy, the shift of peak position, between the calculated results and experimental data, may be due to the fact that the optical potential parameters for the p+^{16}O instead of the p+^{18}O reaction are applied in the model calculation. For ^{112}Cd(p,2n)^{111}In, the theoretical results are in good agreement with the existing experimental data in Fig. 4. The comparison of calculated results with the experimental data for ^{66}Zn(p,n)^{66}Ga, ^{67}Zn(p,n)^{67}Ga, ^{68}Zn(p,n)^{68}Ga and ^{nat}Zn(p,X)^{67}Ga reaction cross sections are given in Fig 5-8, respectively. Our calculated results are in good agreement with experimental data in spite of employing the same optical potential for all ^{64}Zn, ^{66}Zn, ^{67}Zn and ^{68}Zn. In order to evaluate ^{nat}Zn in Fig. 8, we use the following relation :

$$\sigma(^{nat}\text{Zn}) = 0.486 * \sigma(^{64}\text{Zn}) + 0.279 * \sigma(^{66}\text{Zn}) + 0.041 * \sigma(^{67}\text{Zn}) + 0.188 * \sigma(^{68}\text{Zn}).$$

The calculated cross section for ^{nat}Zn(p,X)^{67}Ga is in good agreement with that of the experimental data.

In conclusion, the purpose of our work is not to find optimum optical parameters, but to examine the applicability of the optical potentials in RIPL without any modification of them. Although our evaluated results from model calculations are in agreement with experimental data, we can not announce that our results are excellent and recommend those values yet. It is difficult to find an optical potential for A<40 that varies smoothly with E, because of the low density of scattering states and the big energy gap between two shells in light nuclei. Our evaluations in light nuclei are not in good agreement with the experimental data. For Zn-nuclei with the global optical parameters of Varner *et al.*, we have good agreement with the experimental data. Therefore, the model calculation with the optical potential parameters of Varner *et al.* is a good way to obtain the production cross section in A$\geq$40. There are two tasks next times. First, we will find the optical parameters by ourselves. Second, we will consider effectively the direct interaction and pre-equilibrium effects as well as the compound nucleus effects.

Acknowledgements

References

[1] Soo Youl Oh, Y.X. Zhuang and Jonghwa Chang,*Proceedings of the Korean Nuclear Society Spring Meeting Vol I*, 157-162 (1998); Y. X. Zhuang, in "*The Charged-Particle Cross Section Database for Medical Radioisotope Production*", Calculation Note NDL-03/98, NDL-08/98, NDL-14/98, NDL-17/98, NDL-19/98, NDL-22/98, KAERI (1998).

[2] Doohwan Kim, in "*Evaluation of Proton Induced Reaction on ^{16}O from 0.5 to 50 MeV using ECIS96-GNASH*", Calculation Note NDL-37/98, KAERI (1998); in "*Calculation and Evaluation of Proton-Induced Reactions on ^{14}N, ^{18}O and $^{nat,64,66,67,68}Zn$ up to 50 MeV*", Calculation Note NDL-02/99, KAERI (1999); in "*Calculation and Evaluation of Proton-Induced Reactions on ^{77}Se, ^{112}Cd, ^{127}I, $^{nat,63,65}Cu$, $^{nat,69,71}Ga$, $^{nat,82,83,84,86}Kr$ and $^{nat,85,87}Rb$ up to 50 MeV*", Calculation Note NDL-08/99, KAERI (1999).

[3] A. J. Koning, O. Bersillon and J.-P. Delaroche, in "*JEEF Specialists' Meeting on Intermediate Energy data*", June 18 1997.

[4] J. Raynal, in "*Notes on ECIS94*", Note CEA-N-2772 (1994).

[5] J. Raynal, in "*Proceedings of a Specialists Meeting on the Nucleon-Nucleus Optical Model up to 200 MeV*", 13-15 November 1996.

[6] J. Kopecky and M. Uhl, Phys. Rev. **C42**, 1941 (1990).

[7] J. Kopecky, in "*5. Gamma-Ray Strength Functions : Handbook for calculations of nuclear reaction data Reference input parameter library*", IAEA-TECDOC-1034, August 1998. (WWW-address:http://www-nds.iaea.or.at/ripl)

[8] P. G. Young, in "*4. Optical Model Parameters : Handbook for calculations of nuclear reaction data Reference input parameter library*", IAEA-TECDOC-1034, August 1998. (WWW-address:http://www-nds.iaea.or.at/ripl)

[9] G. R. Satchler, in "*Introduction to Nuclear Reaction*", 2nd Edition ,Oxford University Press (1990).

[10] R. L. Varner et al., in "*A Global Nucleon Optical Model Potential*", Phys. Rep. **201**, 57-119 (1991).

[11] C. Kalbach, Phys. Rev. **C37**, 2350 (1988).

[12] A.V. Ignatyuk, G.N. Smirenkin, and A.S. Tishin, Sov. J. Nucl. Phys. **21**, 255 (1975).

[13] M. B. Chadwick and P. G. Young, in "*Proceedings of International Particle Therapy Meeting and PTCOG XXIV*", 24-26 April 1996.

[14] M.B. Chadwick and P.G. Young, Nucl. Sci. Eng. **123**,17 (1996).

[15] V. Avrigeanu, P.E. Hodgson and M. Avrigeanu, Report OUNP-94-02 (1994); Phys. Rev. **C49**, 2136 (1994).

[16] J. Bojowald *et al.*, Phys. Rev. **C38**, 1153 (1988).

[17] F. D. Becchetti Jr. and G.W. Greenlees, Ann. Rept. J.H.Williams Lab., Univ. Minnesota(1969).

[18] J.J. Menet *et al.*, Phys. Rev. **C4**, 1114 (1971).

[19] S. Igarasi, Japan At. Ener. Res. Insti. **1228**, 41 (1973).

[20] Nuclear Data Evaluation Lab, "*Table of the Nuclides*", :KAERI (WWW-address : http://hpngp01.kaeri.re.kr /CoN/index.html) , KAERI/GP-106/95

	E1	GW1	E2	GW2
p+^{14}N	20.6	4.3	23.5	4.5
p+^{16}O	24.5	6.2	-	-
p+^{18}O	24.5	6.2	-	-
p+^{nat,64,66,67,68}Zn	16.23	3.27	19.19	5.98
p+^{112}Cd	15.81	6.22	-	-

Table 1: The position and width of giant resonance parameters for γ-transion

	proton	neutron	α-particle	deutron	trition or ^{3}He
p+^{14}N	4016	16	9600	6400	8100(He)
p+^{16}O	4017	17	9600	6400	7100(T)
p+^{18}O	4102	200	9600	6400	7100(T)
p+^{nat,64,66,67,68}Zn	5100	2100	9600	6400	7100(T)
p+^{112}Cd	5100	2100	9600	6400	7100(T)

Table 2: The optical parameters list

	$0 \leq E \leq 20$	$20 \leq E \leq 21.95$	$21.95 \leq E \leq 70$
r_v	1.25	1.197	
a_v	0.65	0.593	
V	56.673 - 0.55 * E	53.73 -0.29*E	
r_{wd}	1.25	1.388	
a_{wd}	0.47	0.449	
W_d	13.5	8.64 - 0.145*E	
r_w	1.388		
a_w	0.449		
W	0.0		-5.86 + 0.267*E
r_{vso}	1.25	1.01	
a_{vso}	0.65	0.5	
V_{so}	7.5	6.0	
r_c	1.25	1.2	

Table 3: The optical parameter for p+^{14}N

	proton	neutron
r_v	1.16	$1.16+0.6*A^{\frac{1}{3}}$
a_v	0.75	0.62
V	$49.9\text{-}0.22*E+26.4*\frac{N-Z}{A}$	$46.0\text{-}0.25*E$
r_{wd}	1.37	$1.16+1.1*A^{\frac{1}{3}}$
a_{wd}	0.74-0.008*E	0.35
W_d	$4.2\text{-}0.05*E+15.5*\frac{N-Z}{A}$	7.0
r_w	1.37	$1.16 + 0.6 *A^{\frac{1}{3}}$
a_w	0.74-0.008*E	0.62
W	1.2+0.09*E	0.0+ 0.0004*E
r_{vso}	1.064	$1.16 + 0.6*A^{\frac{1}{3}}$
a_{vso}	0.78	0.62
V_{so}	6.04	7.0
r_c	1.25	0.0

Table 4: The optical parameters for ^{18}O

| Parameter	Value	Uncertainty	Parameter	Value	Uncertainty
V_0	52.9 MeV	$\pm$ 0.2	W_{v0}	7.8 MeV	$\pm$ 0.3
V_t	13.1 MeV	$\pm$ 0.8	W_{ve0}	35 MeV	$\pm$ 1
V_e	-0.299	$\pm$ 0.004	W_{vew}	16 MeV	$\pm$ 1
r_0	1.250 fm	$\pm$ 0.002			
$r_0^{(0)}$	-0.225 fm	$\pm$ 0.009	W_{s0}	10.0 MeV	$\pm$ 0.2
a_0	0.690 fm	$\pm$ 0.006	W_{st}	18 MeV	$\pm$ 1
			W_{se0}	36 MeV	$\pm$ 2
r_c	1.24 fm	-	W_{sew}	37 MeV	$\pm$ 2
$r_c^{(0)}$	0.12 fm	-			
			r_w	1.33 fm	$\pm$ 0.01
V_{so}	5.9 MeV fm^2	$\pm$ 0.1	$r_w^{(0)}$	-0.42 fm	$\pm$ 0.03
r_{so}	1.34 fm	$\pm$ 0.03	a_w	0.69 fm	$\pm$ 0.01
r_{so}^0	-1.2 fm	$\pm$ 0.1			
a_{so}	0.63 fm	$\pm$ 0.02			

Table 5: Parameters of the global nucleon-nucleus optical potential
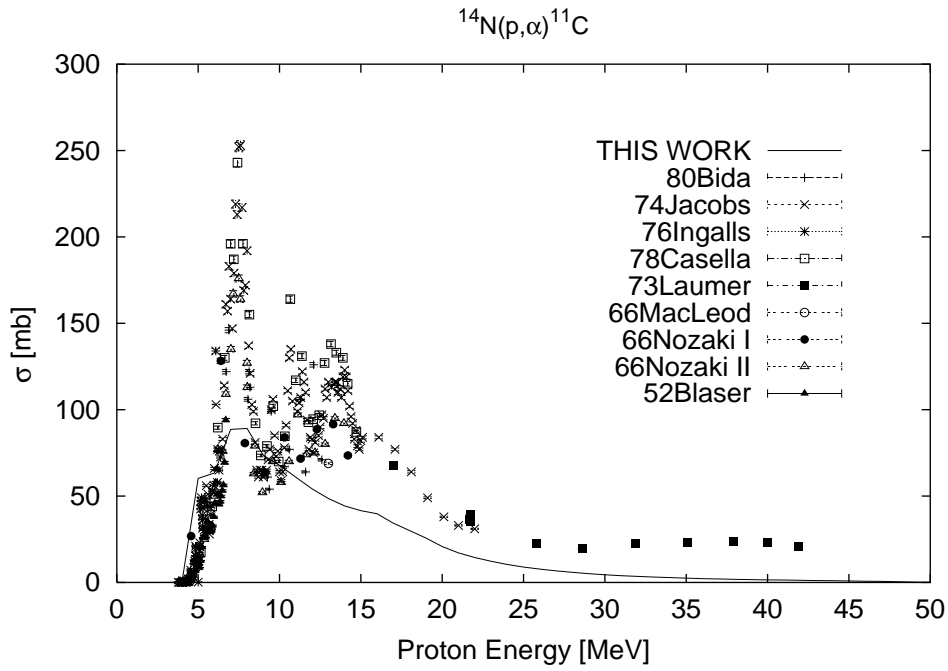
Figure 1: Production cross section on ^{14}N(p,α)^{11}C

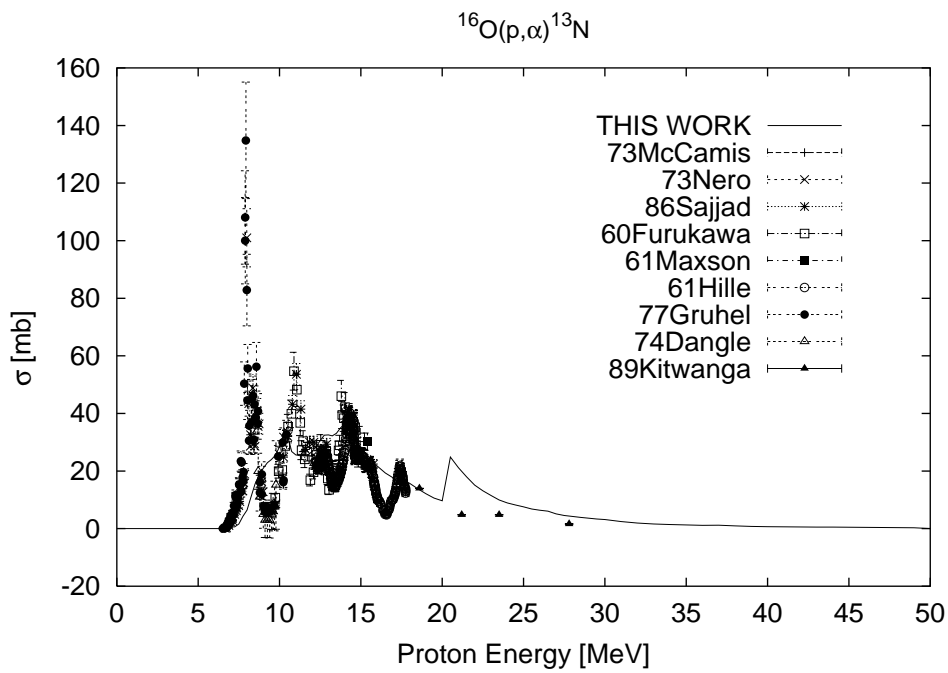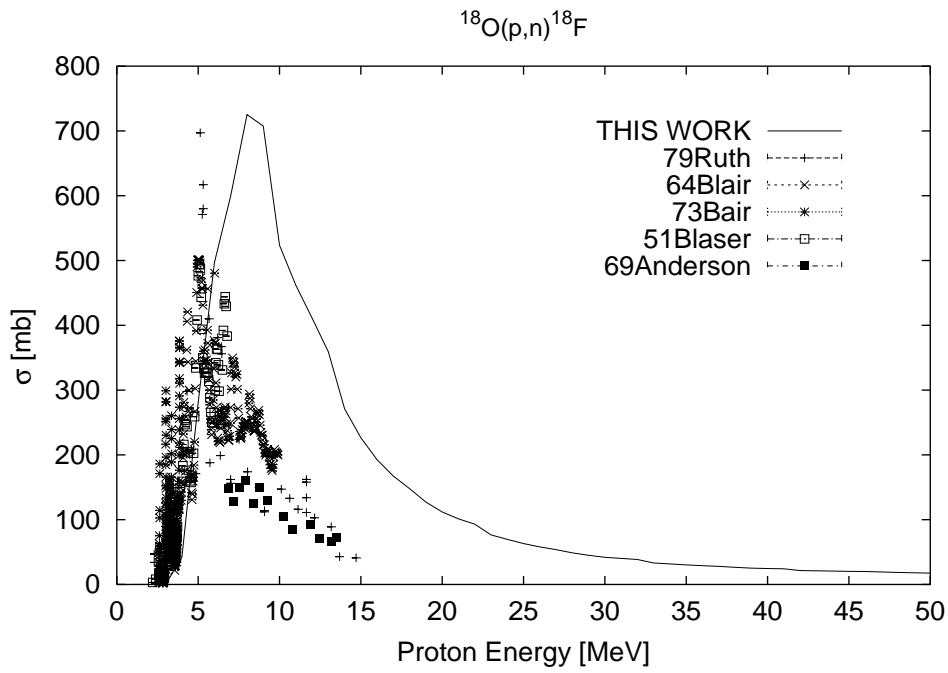Figure 2: Production cross section on ^{16}O(p,α)^{13}N
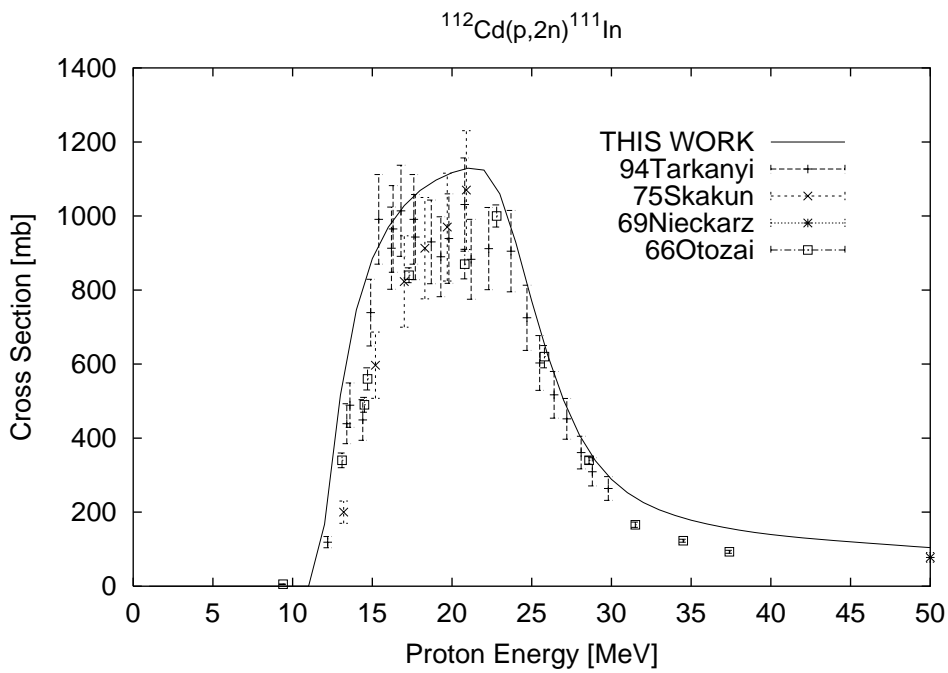
Figure 3: Production cross section on $^{18}O(p,n)^{18}F$

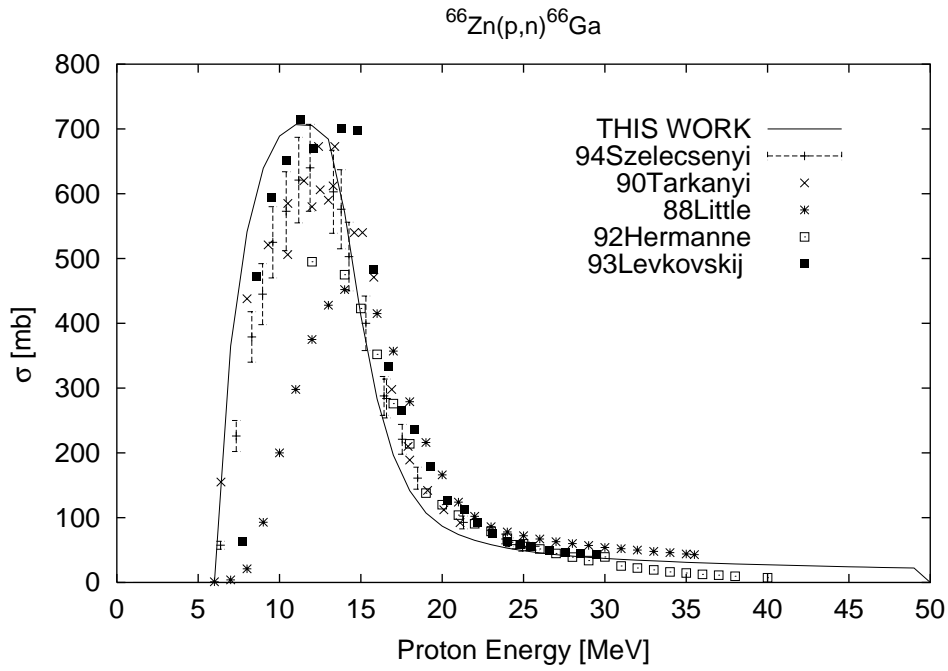Figure 4: Production cross section on $^{112}Cd(p,2n)^{111}In$
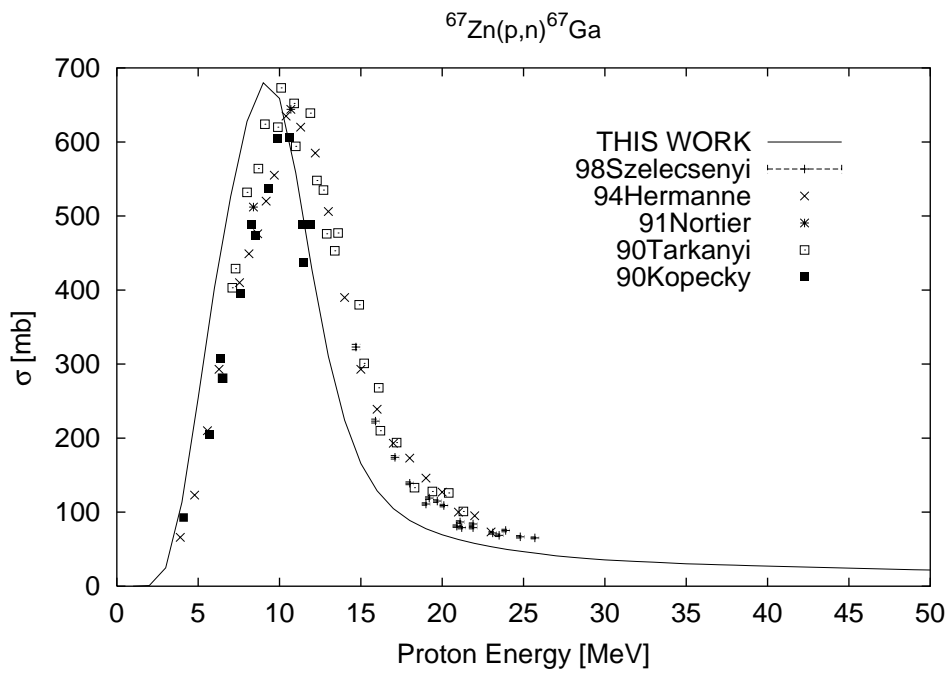
Figure 5: Production cross section on ^{66}Zn(p,n)^{6}Ga
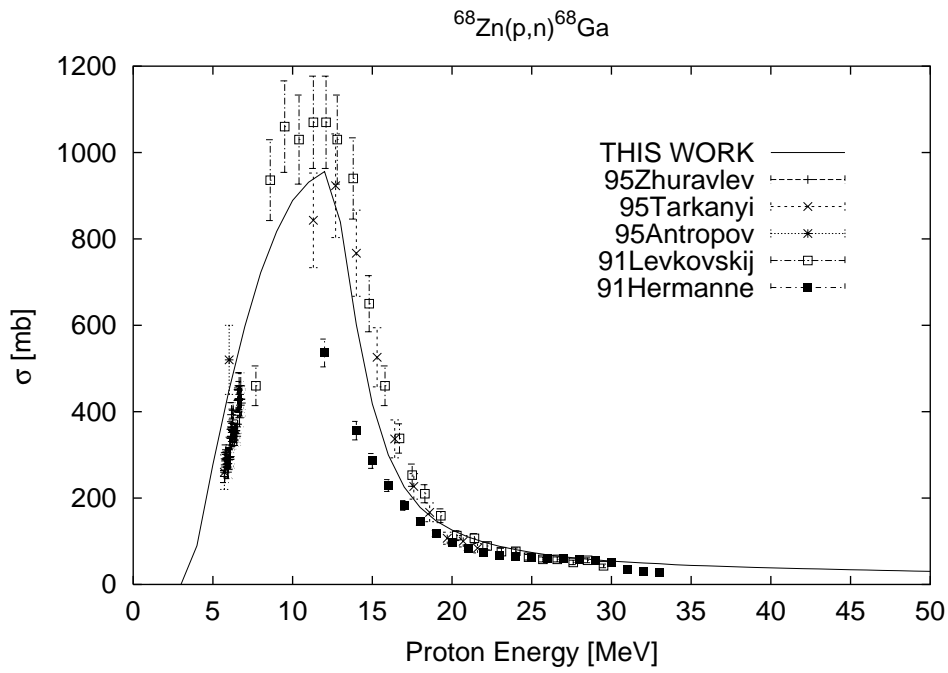

Figure 6: Production cross section on ^{67}Zn(p,n)^{67}Ga

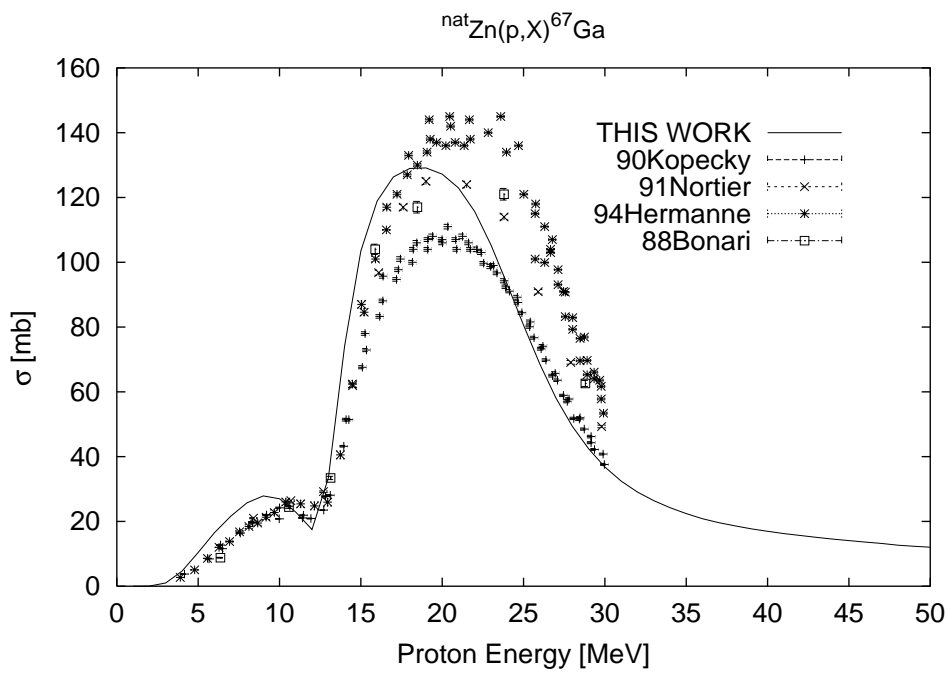Figure 7: Production cross section on ^{68}Zn(p,n)^{68}Ga

Figure 8: Production cross section on ^{nat}Zn(p,X)^{67}Ga